Technologies for
Lightweight Structures

Characterization of the interlaminar fracture toughness of unidirectional thermoplastic composites

<u>Jakob Schmidt</u>[1], Marcus Klingelhöfer[1], Jörg Kaufmann[1], Holger Cebulla[1], Lothar Kroll[2]

[1]   Department of Textile Technologies, jakob.schmidt@mb.tu-chemnitz.de,
      marcus.klingelhoefer@mb.tu-chemnitz.de, joerg.kaufmann@mb.tu-chemnitz.de,
      holger.cebulla@mb.tu-chemnitz.de, Chemnitz University of Technology, Reichenhainer Straße 70,
      09126 Chemnitz, Germany

[2]   Department of Lightweight Structures and Polymer Technology, slk@mb.tu-chemnitz.de,
      Chemnitz University of Technology, Reichenhainer Straße 31/33, 09126 Chemnitz, Germany

Keywords

Double Cantilever Beam, Interlaminar Fracture Toughness, Numerical Analysis, Thermoplastic Composite, Virtual Crack Closure Technique

Abstract

In this study, the critical energy release rate in mode I (G_{1c}) for thermoplastic composites made of carbon fiber (CF) and glass fiber (GF) with a polyamide 6 (PA6) matrix is investigated. Double cantilever beam (DCB) was used as the specimen for the mode I test, and the ASTM D 5528-13 was chosen as standard. Moreover, different methodological approaches were applied by comparing different data reduction schemes from the ASTM D 5528-13 and further analytic approaches from the literature. In addition to the conducted experiments, a numerical model of the DCB test is developed and the virtual crack closure technique (VCCT) is performed on the numerical model to determine G_{1c} for PA6-CF and PA6-GF. For the interlaminar fracture toughness G_{1c} a value of 2.87 mJ/mm^2 was determined for PA6-GF and a value of 2.16 mJ/mm^2 for PA6-CF, which indicate that the use of PA6 as matrix in a composite structure leads to good resistance to damage. A comparison of the different methodological approaches showed a good agreement between the analytical approaches from the literature and the ASTM D 5528-13. In contrast, the values generated for G_{1c} by the VCCT method were significantly higher than those of the other methods.

1   Introduction

Fiber reinforced plastic (FRP) consisting of glass or carbon-fiber reinforcement can be found in a wide range of applications, where the ratio from stiffness to weight or toughness to weight has a high impact on the performance of a product. In comparison to isotropic materials, such as metals, FRP and their distinct microstructure often leads to an anisotropic stiffness and toughness behavior. The classical lamination theory is used to describe this behavior in the linear-elastic region. In addition, various failure criteria are established in the literature, e.g. Puck, Hashin, or Cuntze, which can be used to predict the first ply failure in the composite [1] [2] [3]. The classical failure theories can also be used to calculate the failure up to the last ply. However, these theories are not capable of independently taking into account the energy dissipation processes in the microstructure of the composite as a result of damage. If not only the first ply failure is important in the development of fiber-plastic composite components, but also the exact predictions regarding the failure development in the composite, models of the damage evolution can be used. A possible approach to describe the damage evolution in composite materials is a progressive damage model (PDA) based on continuum damage mechanics (CDM). The proof that the PDA can predict the damage behavior of FRP with a small error has already been carried out on perforated laminate samples [4] and complex composite structures [5]. The benefit of this model is, that the stiffness reduction during the damage evolution of a composite part is based on a damage variable, which takes the distinct failure that occurs in the microstructure of the composite, such as fiber cracking

or matrix cracking, into account [6]. To use PDA in a finite-element analysis software as Ansys or Abaqus certain material properties are needed. These material properties are the critical energy release rates for fiber breaking and matrix breaking under tension or pressure. These material parameters can be obtained in two different ways. On the one hand, the characteristic values can be determined by adapting a simulation to a real test using Design of Experiments and Direct Optimization [6]. On the other hand, some of the required parameters can be determined using standardized procedures provided by the American Society for Testing and Materials (ASTM). One of these standards is ASTM D 5528, which deals with the determination of the critical energy release rate G_{1c} for the delamination process. This value, also known as interlaminar fracture toughness, has already been determined in various papers for FRP based on an epoxy resin. For example, a study of Huang et al. from the year 2020 predicts a G_{1c} value of 0.13 mJ/mm^2 for carbon fiber reinforced epoxy composites [7]. Another study by Barikani et al. investigates the influence of the carbon fiber type and the curing process on the interlaminar fracture toughness and determines values in a range of 0.14 and 0.33 mJ/mm^2 [8]. In contrast, there are only a few studies that deal with the recording of the interlaminar fracture toughness for thermoplastic FRPs. One of these reported in ASTM D 5528 and was determined in the round robin test for carbon fiber reinforced polyetheretherketone (PEEK-CF). A maximum value of 1.72 mJ/mm^2 could be determined for PEEK-CF [9]. In addition, there are no publicly available values for fiber reinforced PA6. However, it is precisely this material combination that offers great potential when it comes to the efficient production of structurally high stressed FRP components in large-scale production [10]. For this reason, the critical interlaminar energy release for fiber-reinforced PA 6 is determined in this publication. The two widespread fiber materials glass and carbon are used as reinforcements for the investigation. The procedure for determining G_{1c} is described in detail in ASTM D 5528, but the standard has several calculation approaches, which, in case of doubt, also lead to different results. In addition, the standard can also be supplemented with other approaches from the literature, which further increases the variety of results. For this reason, the second aim of this publication is to provide an overview of different approaches and to compare the results.

2 Material and Methods

2.1 Materials

The tests in this study are carried out with two differently long fiber reinforced unidirectional (UD) tapes with a matrix made of polyamide 6. One of them is glass fiber reinforced polyamide (PA6-GF) and the other is carbon fiber-reinforced polyamide 6 (PA6-CF). Based on these UD tapes, unidirectional organic sheets measuring 260x260 mm were produced in a hydraulic press. The number of layers, fiber orientation, fiber volume fraction φ, and thickness of the organic sheet h_{DCB} made of PA6-CF and PA6-GF are described in Table 1.

Table 1: Overview over the organic sheets

	Number of layers	φ	h_{DCB}	Fiber orientation
PA6-CF	38	48 %	5.37 mm	0°
PA6-GF	30	47 %	5.73 mm	0°

2.2 Sample preparation based on the ASTM D 5528

To determine the interlaminar fracture toughness G_{1c}, the ASTM D 5528 uses a special specimen design that is called Double-Cantilever-Beam (DCB). The shape of the specimen is shown in Figure 1 and is characterized by an artificial crack with the length a_0, that is already generated during the manufacturing process. To implement the artificial crack, a polytetrafluoroethylene (PTFE) film with a thickness of 0.25 mm is placed in the layer structure before pressing after layer 15 for PA6-GF or 19 for PA6-CF. The samples are taken from the organic sheets using water jet cutting. An overview of the final mean dimensions of the samples for the length l_{DCb}, width b_{DCB}, and length of the artificial crack a_0 is summarized in Table 2. The mean values given in Table 2 are based on four samples per material.

Before sample preparation and testing, drying took place at 80 °C for 24 hours to ensure a moisture content of 0.2 % in the samples. To accommodate the DCB samples in a tensile testing machine, metal blocks were glued to the samples, as shown in Figure 1. The dimensions of the blocks are also presented in Table 2.
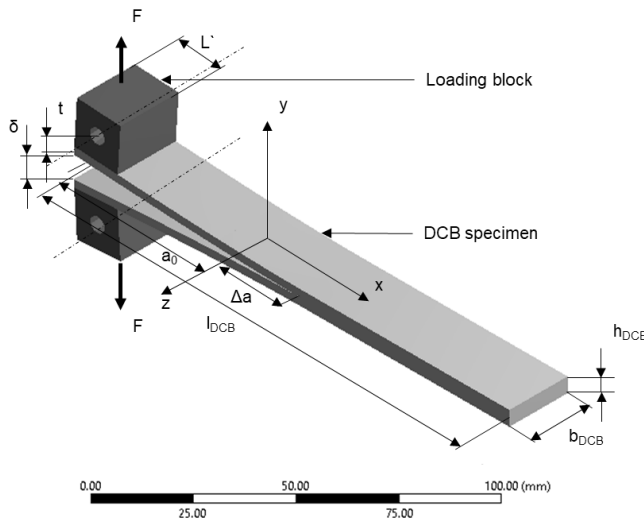

Figure 1: DCB specimen

Table 2: Dimensions of the DCB specimen in mm

	l_{DCB}	b_{DCb}	a_0	L`	t
PA6-CF	179.80	20.04	44.78	15.98	10.68
PA6-GF	179.75	20.06	48.98	15.98	10.86

2.3 Instruments and test procedure

A tensile testing machine with the designation Zwick / Roell Z100 from the Zwick / Roell Group is used to carry out the tests according to ASTM D 5528 and to record the test force F and the traverse path δ, as shown in Figure 1. The crack length Δa, which increases during the test, is recorded by a camera system from GOM GmbH a ZEISS Company. The data F, δ, and Δa obtained through the measurement are synchronized and smoothed by applying a Python script. The smoothing of the data is necessary because the camera system occasionally detects incorrect crack lengths during the measurement. The test speed is set at 20 mm/min.

2.4 Determining the interlaminar fracture toughness based on ASTM D 5528

ASTM D5528 describes four calculation approaches for determining G_1 from the collected data F, a, and δ, whereas a corresponds to the total crack length from combining a_0 and Δa. These approaches can be divided into processes that carry out a direct evaluation using the test force F and those that determine G_{1c} by means of the compliance C, which corresponds to δ / F. The approaches based on the test force are called:

- Beam Theory (BT), which is calculated as follows:

$$G_1 = \frac{3}{2}\frac{F\delta}{b_{DCB}a} \tag{1}$$

- Modified Beam Theory (MBT), which is calculated as follows:

$$G_1 = \frac{3}{2} \frac{F\delta}{b_{DCB}a+|\Delta|} \tag{2}$$

The approaches based on the compliance are called:

- Compliance Calibration (CC), which is calculated as follows:

$$G_1 = n \frac{F\delta}{2b_{DCB}a} \tag{3}$$

- Modified Compliance Calibration, which is calculated as follows:

$$G_1 = n \frac{F\delta}{2b_{DCB}a} \tag{4}$$

The missing quantities Δ, n, and A_1 in equations 2, 3, and 4 will be determined using the method of ASTM D 5528 based on C and a.

In addition to the different calculation methods, ASTM D5528 suggests various evaluation methods. In this work, two evaluation methods are considered. One of them is at the end of the linear-elasticity in the load-displacement diagram $F(\delta)$ and represents the initial value for crack growth. Therefore, it will be named end of linear elasticity (EOLE). The other evaluation method takes into account all data points after reaching the maximum load until the end of a test. Based on this data set, an average value is calculated using the arithmetic mean. For this reason, this method is abbreviated as AV (average value).

2.5 Determining the interlaminar fracture toughness based on other analytic methods

In addition to the methods from ASTM D 5528, two further analytical methods are frequently mentioned in the literature. One of them is the area method (AM), in which G_{1c} is determined via a triangle spanned by the vectors v_1 and v_2 in the $F(\delta)$ diagram, as shown in Figure 2 [11].
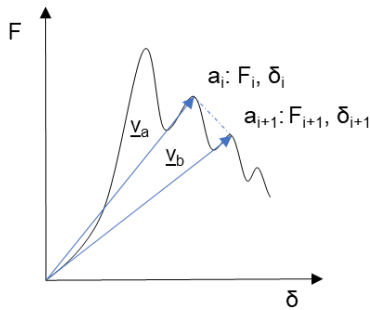

Figure 2: Area method

In addition to AM, Kaveh describes a process that treats the open ends of the DCB sample like clamped bending beams. Based on the assumption of an ideal bending line and knowledge of the Young's modulus in the fiber direction E_{11}, the length of the crack a can then be calculated as follows [12]:

$$a = \sqrt[3]{\frac{3}{2}\left(\frac{\delta E_{11}I}{F}\right)} \tag{5}$$

This calculated crack length a can then be used in one of the ASTM methods, equation 1-4, or the area method. In this work equation 1 is used for further evaluation according to Kaveh. This method is abbreviated as KA.

2.6 Determining the interlaminar fracture toughness with numerical methods

A numerical method for determining G_{1c} is the finite element method (FEM). For this, the test setup must be simulated virtually. In this study, the FEM program Ansys is used to create a virtual test environment of the ASTM D 5528, shown in Figure 3a. Ansys, in its version 2021 R 1 offers various models to predict crack growth for applied external forces or displacements on a DCB specimen. One of them is the interface delamination in combination with the virtual crack closure technique (VCCT) [13]. To use this approach, the layer in which the crack growth will occur must be meshed with interface 205 elements, shown in Figure 3b. During the calculation, G_1 at the crack front is determined with the VCCT. If G_1 reaches a specified G_{1c} value, crack growth occurs in the simulation. Based on this, the numerically calculated values for the test force F can be adapted to those measured in the real experiment with a given δ. For the VCCT and the interface delamination the boundary conditions, shown in Figure 3c, are used. The element length for the mesh, shown in Figure 3d, is determined by a parameter study. It was investigated that halving the element length from 3 mm only leads to a change of 1.3 % in the results, with the calculated test force serving as a reference. Taking this into account, an element length of 3 mm is used in this study. The time step sizing during crack growth is set to 0.001 s, based on the work by Gliszczynski et al. [14].
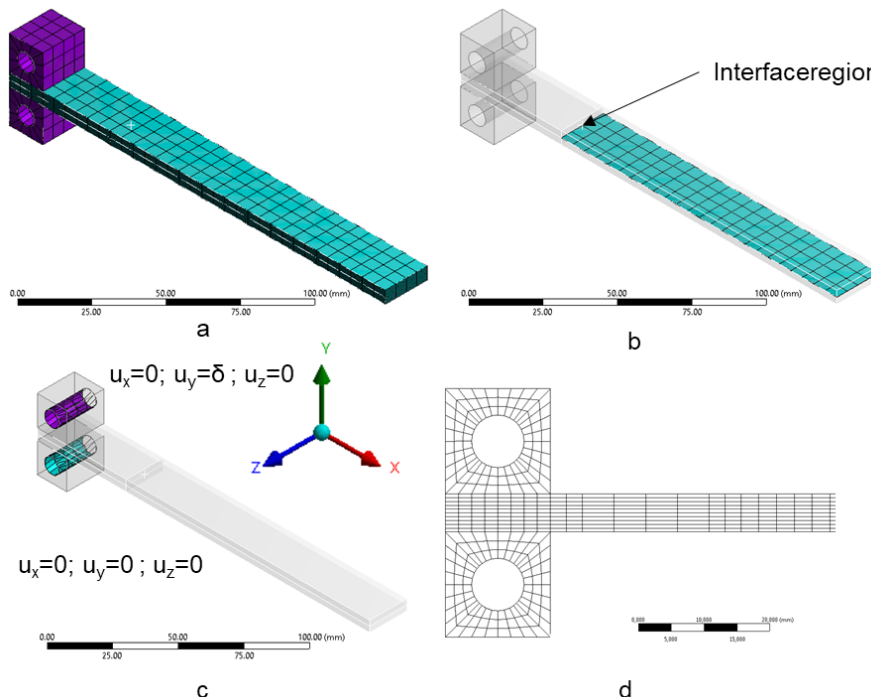

Figure 3: Virtual test environment of the DCB specimen

3 Results

Comparing the graphs for two representative samples of each material qualitatively (Figure 4), the following statements can be made:

- The sawtooth profile in the F(δ)-diagram of PA6-CF suggests sudden crack growth.
- The F(δ)-diagram of PA6-GF suggests a more continuous crack growth.
- With the samples made of PA6-CF, sudden failure occurs along the undamaged remaining area at a certain crack length around 80 mm.

Comparing the materials PA6-CF and PA6-GF based on the averaged maximum test force, the following can be recorded:

- The mean maximum test force for PA6-CF is 332.82 N with a standard deviation of 5.1 %.

- The mean maximum test force for PA6-GF is 231.40 N with a standard deviation of 9.8 %.
- Thus, the mean maximum test force of PA6-CF exceeds that of PA6-GF by 43.8 %.
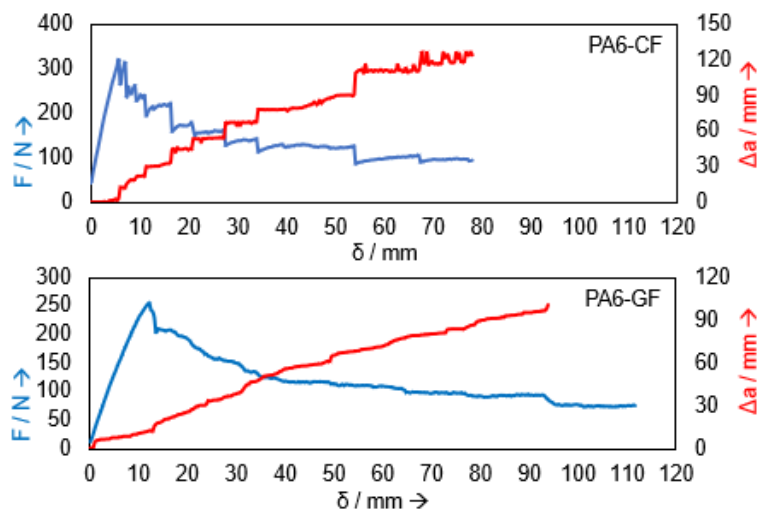

Figure 4: Load-crack length-displacement diagram of PA6-CF and PA6-GF

If the materials are not compared based on the maximum test force, but rather based on the interlaminar fracture toughness, this leads to different results.
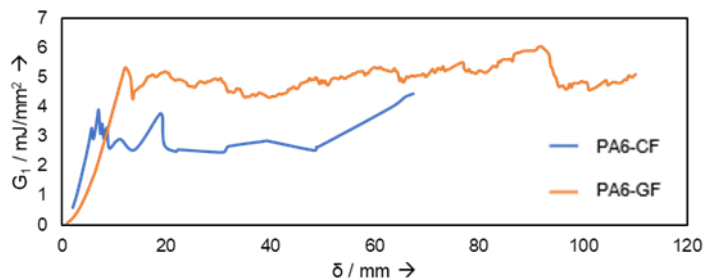

Figure 5. Interlaminar fracture toughness-displacement diagram

Therefore, Figure 5 shows the $G_1(\delta)$-diagram for two representative samples of each material. The maximum achieved value of G_1 for PA6-GF clearly exceeds that of PA6-CF. However, the exact amount of the difference is heavily dependent on the evaluation method chosen. This is underlined by Table 3. Table 3 summarises the median values of all calculation approaches from ASTM D 5528 for the evaluation at the end of linear elasticity (EOLE) and averaged values for G_{1c} over all data points (AV). In addition, the difference between the minimum and maximum median values between the calculation methods are emphasized (max-min). Depending on the calculation approach, these max-min values can be up to 30 % of the results.

Table 3: Test results based on the methods of the ASTM D 5528 in mJ/mm^2

	EOLE		AV	
	PA6-CF	PA6-GF	PA6-CF	PA6-GF
BT	2.87	3.27	3.20	4.35
MBT	2.16	2.87	3.02	3.71
CC	2.62	3.10	2.98	3.63
MCC	2.86	3.36	3.10	4.26
Max-min	0.71	0.49	0.22	0.72

If the materials are compared based on the conservative values within a calculation approach and evaluation point, using the MBT at the evaluation point ELEO, this results in a value of 2.16 mJ/mm^2 for PA6-CF and 2.87 mJ/mm^2 for PA6-GF. If all relevant data points are considered in form of the average value (AV), the most conservative case under the consideration of the MBT leads to G_{1c} values of 3.02 mJ/mm^2 for PA6-CF and 3.71 mJ/mm^2 for PA6-GF. When using the other evaluation methods from the literature, the higher G_{1c} value of PA6-GF compared to PA6-CF is confirmed, as shown in Figure 6. In Figure 6, the MCC approach from ASTM D 5528 in combination with the AV evaluation is compared to the methods from the literature based on the median value. It can be concluded, that both the AM method and the method according to Kaveh lead to a good agreement with the methods from the ASTM, as shown in Figure 6. The differences between the calculation approaches from the literature, AM, and Kaveh, with the MCC approach from the ASTM are not greater than the differences between the methods in the ASTM itself. In contrast, the VCCT method does not lead to a good agreement with the calculation approaches from the ASTM (Figure 6). The numerically calculated value for G_{1c} using VCCT is 73.12 % above the calculated results from the ASTM for PA6-CF and 39.42 % for PA6-GF.
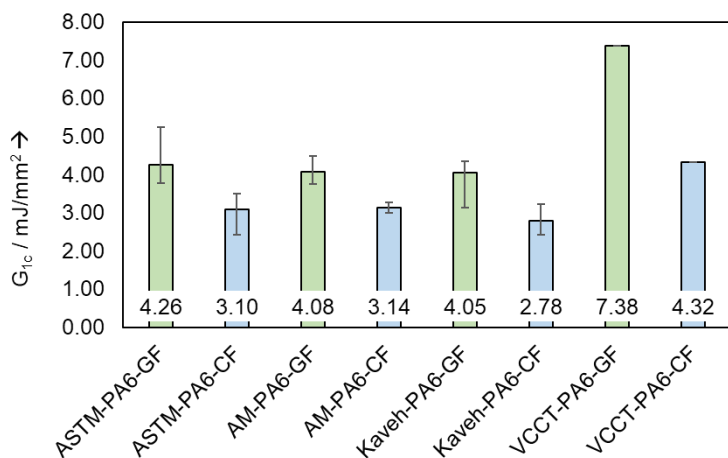

Figure 6: Comparison of calculation approaches from the literature and the ASTM D 5528

4   Discussion and conclusion

In this study, the interlaminar fracture toughness for various fiber materials were determined in mode I for FRP based on a matrix of PA 6. Various methods from ASTM D 5528 and the literature for calculating G_{1c} were used and compared with one another. If the most conservative values from the results for G_{1c} are used, this leads to a value of 2.16 mJ/mm^2 for PA6-CF and 2.87 mJ/mm^2 for PA6-GF.

Based on these results, it can be assumed that the glass fiber reinforcement led to an increase in the interlaminar fracture toughness. However, it has to be considered that UD tapes from different material manufacturers were used for the tests and therefore the composition of the polymer matrix might differ.

Nevertheless the values for fiber reinforced PA6 are well above the values of G_{1c} for FRP with epoxy resin or PEEK matrix, which were determined in previous studies [7] [9] [14]. In addition, it was found that the results from the area method and the calculation method according to Kaveh are in good agreement with the results from the ASTM D 5528. However, the application of the VCCT did not lead to a good agreement between these results. This finding contradicts previous work by Gliszczynski et al., which was carried out on carbon fiber reinforced epoxy resin samples and showed good agreement between the VCCT method and the experimentally collected data [14]. An explanation could be the significantly higher test forces in the presented paper and the behaviour of the PA6 matrix. To overcome this problem, the VCCT could be replaced by the application of a cohesive zone model in future work. In addition, the exact influence of the matrix material should be investigated by using an equivalent composition of the PA6.

Acknowledgements

References

[1]   ASTM D 5528-13.: Standard Test Method for Mode I Interlaminar Fracture Toughness of Unidirectional Fiber-Reinforced Polymer Matrix Composites. West Conshohocken, 2013, PA: ASTM International. doi:10.1520/D5528-13

[2]   Ansys Inc. ANSYS Mechanical APDL Fracture Analysis Guide. Canonsburg, PA.

[3]   Barbero, E.; Shahbazi, M.: Determination of Material Properties for ANSYS Progressive Damage Analysis of Laminated Composites. o Composite Structures, 176 (2017), pp. 768–779. doi:10.1016/j.compstruct.2017.05.074

[4]   Barikani, M.; Saidpour, H.; Sezen, M.: Mode-I Interlaminar Fracture Toughness in Unidirectional Carbon-fiber/Epoxy Composites. Irianian Polymer Journal, 11 (2002), pp. 413-423.

[5]   Cuntze, R.; Deska, R.; Szelinski, B.; Jeltsch-Fricker, R; Meckbach, S.; Huybrechts, D.; Kopp, J.; Kroll, L.; Rackwitz, R.; Gollwitzer, S.: Neue Bruchkriterien und Festigkeitsnachweise für unidirektionalen Faserkunststoffverbund unter mehrachsiger Beanspruchung - Modellbildung und Experimente. Düsseldorf: VDI Verlag GmbH, 1997.

[6]   Gliszczynski, A.; Samborski, S.; Rzeczkowski, J.: Mode I Interlaminar Fracture of Glass/Epoxy Unidirectional Laminates. Part II: Numerical Analysis. Materials, 2019, pp. 2-18. doi:10.3390/ma12101604

[7]   Hashin, Z.; Rotem, A.: A fatigue failure criterion for fiber reinforced materials. J. Compos. Mat., 7(4) (1973), pp. 448–464. doi:10.1177/002199837300700404

[8]   Huang, Y.; Liu, W.; Jiang, Q.; Wei, Y.; Qui, Y.: Interlaminar Fracture Toughness of Carbon-Fiber-Reinforced Epoxy Composites Toughened by Poly(phenylene oxide) Particles. Applied Polymer Materials, 2(8) (2020), pp. 3114-3121. doi:10.1021/acsapm.0c00285

[9]   Kashaba, U.; Sebaey, T.; Selmy, A.: Experimental verification of a progressive Experimental verification of a progressive with different clearances. International Journal of Mechanical Sciences, 152 (2019), pp. 481-491. doi:10.1016/j.ijmecsci.2019.01.023

[10] Kaveh, A.: Determining the crack propagation in DCB composite specimens by fiber bridging modeling. Revista Técnica de la Facultad de Ingeniería Universidad del Zulia, 37(2), 2014, pp. 1-9.

[11] Pinho, S.; Robinson, P.; Iannucci, L.: Fracture toughness of the tensile and compressive fibre failure modes in laminated composites. Composites Science and Technology, 66(13) (2006), pp. 2069–2079. doi:10.1016/j.compscitech.2005.12.023

[12] Puck, A., & Schürmann, H.: Failure analysis of FRP laminates by means of physically based phenomenological models. Compos. Sci. Tech. 58, 1998, doi:10.1016/S0266-3538(96)00140-6

[13] Reddemann, J.: Beitrag zum energieeffizienten Einsatz von Thermoplast-CFK. Göttingen: Cuvillier Verlag, 2016.

[14] Subramanyam, N.; Vijayakumar, R.; Prahlada, R.: Prediction of Progressive Damage and Failure Analysis of Rotorcraft Composite Nose Cowling By Continuum Damage Mechanics Model. Materials Today: Proceedings 5(2) (2018), pp. 4335–4344. doi:10.1016/j.matpr.2017.11.699